

1 Incorporating the Wilshire equations for time to failure and the minimum creep
2 rate into a continuum damage mechanics for the creep strain of Waspaloy

3

4 Mark Evans*

5 **Institute of Materials, Bay Campus, Swansea University, Fabian Way, Crymlyn Burrows,*
6 *Wales, SA1 8EN, UK; m.evans@swansea.ac.uk; Tel.: 01792295748. Corresponding author.*

7

8 ABSTRACT: In this paper, a new constitutive model is presented that combines the Wilshire
9 equations with a modified Kachanov-Rabotnov continuum damage mechanics (CDM) to
10 enable the prediction of uniaxial creep curves that contain both a primary and tertiary stage.
11 Another advantage of this approach is that the Wilshire equations have been shown to
12 accurately extrapolate the operational failure times and minimum creep rates from very short-
13 term tests. This approach also removes the need to estimate the Wilshire time to strain
14 equation at numerous different strains. A simple but multi-step procedure is also introduced
15 for estimating the unknown parameters of this model. When applied to Waspaloy data, the
16 model was shown to represent the shape of the experimental creep curves reasonably well
17 (especially at low and high strains) and provides reasonable creep curve predictions – with
18 percentages errors averaging around 4-5%.

19

20 *Keywords:* Creep curves, Wilshire equations, Constitutive models

21

1. Introduction

The introduction of new materials has already supported major improvements in the efficiency and reliability of aeroengines [1]. Nevertheless, a combination of rising energy prices and global warming are now requiring further increases in engine efficiency to minimise fuel consumption and greenhouse gas emissions. One way to achieve this is through higher operational temperatures, but this requires materials with enhanced temperature capabilities such as the Nickel based superalloys – of which Waspaloy, is an example. Unfortunately, the ‘materials development cycle’ currently takes many years [2]. Long duration test programmes are needed to establish the tensile stresses which can be sustained over the planned design lives without creep failure occurring at the temperatures encountered during service. The Wilshire equation for time to failure has great potential for reducing the length of the development cycle because it has been shown in the literature to produce reliable failure time predictions for the operating conditions (or close to) of many materials using only very short term accelerated tests [3-12].

In order to prevent aeroengine blades rubbing against the engines outer casing, strain is also a very important design and material development criteria. Being able to realistically predict strain at given times is also very important for converting small punch test data into equivalent uniaxial test results given that the most promising way of doing this is via finite element models of the punch test. These finite element models require equations yielding incremental increases in strain with time and so require accurate predictions of all points along a uniaxial creep curve. The successful correlation of small punch and uniaxial test results will help release the full potential of the small punch test.

However, the literature is quite sparse on how to modify the Wilshire equations so as to be able to predict times to specified strains and therefore complete creep curves [13-14]. Most recently, Evans and Williams [15] have incorporated Artificial Neural Network technology (ANN) into the Wilshire methodology as a solution. However, the resulting model has no closed form expression and is quite cumbersome to implement. It involves numerous steps including modelling the Wilshire time to strain parameters as a function of strain using ANN’s, entering a strain into these ANN’s to get the Wilshire parameters and finally inserting these Wilshire parameters (and that strain) into the Wilshire time to strain equation to get a prediction for the time to that strain. Repeating for all strains up to the rupture strain yields the predicted creep curve. Such a process is not ideally suited to finite element modelling of the small punch creep test. Cano and Stewart [16] by passed this procedure by integrating the Wilshire equations into a CDM model, but the resulting model was not capable of modelling the primary stages of the creep process. Therefore, the aim of this paper is to overcome the limitations of these last two approaches by integrating the Wilshire equations for time to failure and minimum creep rates into a modified Kachanov-Rabotnov (K-R) creep continuum damage model. These modifications allow for primary creep and for failure to occur when the damage parameter is less than unity.

To achieve this objective the paper is structured as follows. The next section describes the uniaxial creep tests of the polycrystalline Nickel alloy Waspaloy that have been conducted at Swansea University. Section 3 reviews some CDM approaches to creep already in the literature. Section 4 outlines some statistics that can be used for evaluating the effectiveness of a creep model in predicting various creep properties. Section 5 outlines the proposed CDM model to be used in this paper, together with a description of how the unknown parameters of this model can be quantified. This model is then applied to the

72 Waspaloy data in section 6. The main findings are then summarised in the conclusions
73 section.

74

75 **2. The data**

76

77 Thirty-one cylindrical test pieces were machined from an received Waspaloy bar, with
78 a gauge length of 28mm and a diameter of 5mm. The chemical composition of this batch of
79 material is shown in Table 1a. The material was heat treated for 4 h at 1353 K (water
80 quenched), 4 h at 1123 K (air cooled) and 16 h at 1033 K (air cooled). This resulted in a
81 uniform equiaxed structure of average grain diameter 45 μm . The microstructure contained
82 uniform γ' particles of mean diameter 0.3 μm .

83

84 Table 1a Chemical composition (weight %)

Cr	Co	C	Mn	Si	Fe	Mo	Ti	Al	B	Zr	S	P	Cu
19.1	13.5	0.03	0.1	0.1	0.79	4.08	3.15	1.3	0.005	0.07	0.0025	0.01	0.1

Also 5 ppm of Ag, 10 ppm of Pb and 0.5 ppm of Bi with balance Ni.

85

86 The tensile strength (σ_{TS}) values for this batch of material are shown in Table 1b.
87 Normalisation of the stress using the tensile strength is done using these measured UTS
88 values – no equation was required for interpolating the UTS as the test matrix contained no
89 creep curves at any other temperature.

90

91 Table 1b Variation of Tensile Strength with temperature

Temperature (K)	873	923	973	1023
Tensile Strength (MPa)	1154	1120	975	827

92

93 The specimens were tested in tension over a range of stresses at 873K, 923K, 973K
94 and 1023K using high precision in Andrade-Chalmers constant-stress machines [17]. Loads
95 and stresses could be applied and maintained to an accuracy of 0.5%. In all cases,
96 temperatures were controlled along the gauge lengths and with respect to time to better than
97 ± 1 K. The extensometer was capable of measuring tensile strain to better than 10^{-5} . Loading
98 machines, extensometers and thermocouples were all calibrated with respect to NPL traceable
99 standards. At 873K, eight specimens were placed on test over the stress range 1150 MPa to
100 700 MPa, at 923K seven specimens were placed on test over the stress range 1000 MPa to
101 550 MPa, at 973K nine specimens were placed on test over the stress range 950 MPa to 200
102 MPa and at 1023K seven specimens were tested over the stress range 700 MPa to 250 MPa.
103 Up to 400 creep strain/time readings were taken during each of these tests. Because
104 Waspaloy can serve at temperatures up to 920K for critical applications and 1040K for less
105 demanding situations, the test programme covered stress ranges giving creep lives up to
106 5,500 h (around 19852000 s) at 873 to 1023 K. This data set has been published by Wilshire
107 and Scharning [18] and Evans [19].

108

109 Analysis of the data obtained on constant load machines would proceed in the same
110 way as outlined in this paper – all that is required is that the creep curves, minimum creep
111 rates and failure times are all obtained at constant load. Converting the resulting predicted
112 constant load creep curves into constant stress creep curves required for small punch
113 modelling would require further manipulation of the predicted curves.

114 **3. A brief review of some well-known CDM models**

115 *3.1. The Kachanov-Rabotnov (K-R) model*

116 The Kachanov-Rabotnov (K-R) creep continuum damage model at constant
117 temperature consists of a creep strain rate, $\dot{\varepsilon}$, and a damage evolution equation \dot{w} [20,21]

$$118 \quad \frac{dw}{dt} = \dot{w} = \frac{\delta\sigma^\chi}{(1-\phi)(1-w)^\phi} \quad (1a)$$

$$119 \quad \frac{d\varepsilon}{dt} = \dot{\varepsilon} = A \left(\frac{\sigma}{1-w} \right)^n \quad (1b)$$

120 where A and n are the Norton power law constants, σ is the constant stress associated with a
121 uniaxial creep test, w is the K-R damage parameter that varies from 0 through to 1 during the
122 creep test, and δ , χ , and ϕ are the tertiary creep damage constants. The constant χ must be
123 greater than or equal to unity (but is typically set at 3). $\sigma/(1-w)$ is often referred to as the
124 effective stress, representing the accelerating effect of damage accumulation on the initial
125 stress. Assuming that failure occurs when $w = 1$, the definite integral of Eq. (1a) yields an
126 expression for both the time to failure t_f and K-R damage

$$127 \quad t_f = \frac{1}{\delta\sigma^\chi} \quad (1c)$$

$$128 \quad w = 1 - [1 - \delta\sigma^\chi t]^{\frac{1}{\phi+1}} = 1 - \left[1 - \frac{t}{t_f} \right]^{\frac{1}{\phi+1}} \quad (1d)$$

129 If Eq. (1d) is inserted into Eq. (1b) and the indefinite integral taken, the form of the K-
130 R uniaxial creep curve at stress σ and constant temperature emerges

$$131 \quad \varepsilon = \frac{A\sigma^n}{1-\frac{n}{\phi+1}} \left\{ 1 - \left[1 - \frac{t}{t_f} \right]^{1-\frac{n}{\phi+1}} \right\} \quad (1e)$$

132 *3.2. Modified Kachanov-Rabotnov (K-R) model*

133 One issue with the K-R model is that it assumes failure occurs when $w = 1$, which in
134 turn implies that the effective stress, creep rate and rate of damage accumulation are also all
135 infinite at failure – a phenomenon that is not seen in uniaxial creep testing of metals for high
136 temperature applications. This can be tackled within the K-R framework by introducing a
137 critical damage parameter, $w_f \leq 1$, such that failure occurs when w reaches this quantity.
138 Inserting w_f for w into Eq. (1d) when $t = t_f$ and solving for δ gives

$$139 \quad \delta = \frac{1 - [1 - w_f]^{\phi+1}}{\sigma^\chi t_f} \quad (2a)$$

140 which when substituted back into Eq. (1d) gives a modified K-R damage as a function of
141 time

$$142 \quad w = 1 - \left[1 + ([1 - w_f]^{\phi+1} - 1) \frac{t}{t_f} \right]^{\frac{1}{\phi+1}} \quad (2b)$$

143 with the failure time equation remaining unchanged. Clearly, Eq. (2b) collapses to Eq. (1d)
144 when $w_f = 1$. Notice also that Eq. (1b) can be written as

$$w = 1 - \frac{\sigma}{\left(\frac{\dot{\varepsilon}}{A}\right)^{\frac{1}{n}}} = \frac{\left(\frac{\dot{\varepsilon}}{A}\right)^{\frac{1}{n}} - \sigma}{\left(\frac{\dot{\varepsilon}}{A}\right)^{\frac{1}{n}}} \quad (3)$$

so that the K-R model implies that the minimum creep rate, $\dot{\varepsilon}_m = A\sigma^n$, occurs when there is no damage accumulation, i.e. when $w = 0$. This is most clearly seen in Eq. (1d) where when $\dot{\varepsilon} = \dot{\varepsilon}_m$, $\left(\frac{\dot{\varepsilon}}{A}\right)^{\frac{1}{n}} = \sigma$ so that $w = 0$. As soon as the creep strain rate is greater than the minimum creep strain rate, the term $\left(\frac{\dot{\varepsilon}}{A}\right)^{\frac{1}{n}}$ becomes larger than the equivalent stress, σ , and irreversible damage begins. Hence a clear limitation of the K-R model is that it does not account for primary creep.

3.3. The Hayhurst modification of the K-R model

Hayhurst et.al. [22] presented a solution to this problem by introducing a second damage variable – w_2 . In this model the first damage parameter, w , represented dislocation softening and evolves from 0 through to 1. w_2 represented nucleation-controlled creep constrained to evolve from 0 to 1/3. In one version of this model, the creep rate and rate of accumulation in the new damage variable were dependent on stress through use of a hyperbolic sine function. A different approach that does not require the use of this additional damage variable was also proposed by Hayhurst et. al. [23] which simply involves adding the power expression t^m to Eqs. (1a,b) – where m is a material constant

$$\frac{dw}{dt} = \dot{w} = \frac{\delta\sigma^\lambda t^m}{(1-\phi)(1-w)^\phi} \quad (4a)$$

$$\frac{d\varepsilon}{dt} = \dot{\varepsilon} = A \left(\frac{\sigma}{1-w}\right)^n t^m \quad (4b)$$

Assuming that failure occurs when $w = 1$, the definite integral of Eq. (4a) yields an expression for both the time to failure t_f and damage w

$$t_f = \left[\frac{1+m}{\delta\sigma^\lambda}\right]^{\frac{1}{m+1}} \quad (4c)$$

$$w = 1 - \left[1 - \left(\frac{t}{t_f}\right)^{m+1}\right]^{\frac{1}{\phi+1}} \quad (4d)$$

If Eq. (4d) is inserted into Eq. (4b) and the indefinite integral taken, the form of the uniaxial creep curve at stress σ and constant temperature emerges

$$\varepsilon = \frac{A\sigma^n}{\left(1-\frac{n}{\phi+1}\right)(m+1)} \left\{1 - \left[1 - \left(\frac{t}{t_f}\right)^{m+1}\right]^{1-\frac{n}{\phi+1}}\right\} \quad (4e)$$

It is clear from Eq. (4e) that the shape of the creep curve is such that it has a primary and tertiary component due to the fact that t/t_f has two power exponents - $(m+1)$ and $1-n/(\phi+1)$. This modified expression reduces to the original K-R model when $m = 0$, implying that primary creep is picked up via a negative value for m .

3.4. Power Law breakdown

175 The K-R, modified K-R and Hayhurst models discussed above all suffer from power
 176 law breakdown in that the form of the failure time equation is a power law (see Eqs. (1c,4c)
 177 and it is known that the parameter n is then not a material constant but varies with stress.
 178 Hayhurst et.al. [22] started to address this issue by using a Sinh rather than a power law
 179 relation to describe the role of stress on creep strain. More recently, the coupled Sinh creep
 180 damage constitutive model of Haque et. al. [24] consists of a creep strain rate and damage
 181 evolution equation as follows

$$182 \quad \frac{dw}{dt} = \dot{w} = \frac{B[1-e^{-\phi}]\sinh\left(\frac{\sigma}{\sigma_t}\right)^X}{\phi} e^{\phi w} \quad (5a)$$

$$183 \quad \frac{d\varepsilon}{dt} = \dot{\varepsilon} = A\sinh\left(\frac{\sigma}{\sigma_s}\right) e^{\lambda w^{3/2}} \quad (5b)$$

184 where σ_t and σ_s are additional material constant and the parameters in Eqs. (5) have different
 185 meanings to the same parameters in the previously discussed models. Whilst the use of the
 186 Sinh function helps overcome power law breakdown, the definition of λ as $\ln(\dot{\varepsilon}_f/\dot{\varepsilon}_m)$ in Eq.
 187 (5b) means that the creep curves starts at time $t = 0$ with a creep rate equal to $\dot{\varepsilon}_m$ and from
 188 that point on the creep rate continues to increase, i.e. the model is for tertiary creep only ($\dot{\varepsilon}_f$ is
 189 the creep rate at failure).

190 An alternative approach is to overcome power law break down by making use of the
 191 Wilshire equations [3]. These equations have been shown to predict well both failure times
 192 and minimum creep rates over a wide range of stress and temperatures using just accelerated
 193 test data [4-12]. Cano et. al. [16] have recently developed a CDM version of this Wilshire
 194 approach in which they replace the Sinh function in Eqs. (5) with the Wilshire equations

$$195 \quad \frac{dw}{dt} = \dot{w} = \frac{[1-e^{-\phi}]}{\phi} \frac{1}{t_f} e^{\phi w} \quad (6a)$$

$$196 \quad \frac{d\varepsilon}{dt} = \dot{\varepsilon} = \dot{\varepsilon}_m e^{\lambda w} \quad (6b)$$

197 where

$$198 \quad t_f = \frac{\left[\frac{-\ln(\sigma/\sigma_{TS})}{k_1}\right]^{\frac{1}{u}}}{\frac{-Q_c}{e^{RT}}} \quad (6c)$$

$$199 \quad \dot{\varepsilon}_m = \frac{\left[\frac{-\ln(\sigma/\sigma_{TS})}{k_2}\right]^{\frac{1}{v}}}{\frac{Q_c}{e^{RT}}} \quad (6d)$$

200 and u, v are materials constants, σ_{TS} is the tensile strength, R the universal gas constant, Q_c
 201 the activation energy for self-diffusion, and T the absolute temperature. Eqs. (6c,d) are the
 202 Wilshire equations for time to failure and minimum creep rates. In Eq. (6b), λ is set equal to
 203 $\ln(\dot{\varepsilon}_f/\dot{\varepsilon}_m)$ and in Eq. (6a) ϕ is set equal to $\ln(\dot{w}_f/\dot{w}_0)$ where \dot{w}_f/\dot{w}_0 is the ratio of the final to
 204 initial rates of damage accumulation. As such this is once again a model for tertiary creep
 205 only.

206 Another approach to solving the power law issue was presented by Liu and Murakami
 207 [25] who specified the damage rate and creep rate equations as

208 $\frac{dw}{dt} = \dot{w} = \frac{B[1-e^{-\phi}]\sigma^\chi}{\phi} e^{\phi w}$ (7a)

209 $\frac{d\varepsilon}{dt} = \dot{\varepsilon} = A\sigma^n e^{qw^{3/2}}$ (7b)

210 where A, B, q, n, ϕ and χ are again material constants – again with different meanings to
211 those in the K-R model.

212 4. A Proposed CDM models based on the Wilshire equations

213 4.1. Specification

214 First, rewrite the Wilshire equation for the minimum creep rate as

215 $\dot{\varepsilon}_m = \left[\frac{1}{k_{2j}} \right]^{1/v_j} e^{-\frac{Q_{cj}}{RT}} [-\ln(\sigma/\sigma_{TS})]^{1/v_j} = A_j \tau^{n_j}$ (8a)

216 where $A_j = \left[\frac{1}{k_{2j}} \right]^{1/v_j} e^{-\frac{Q_{cj}}{RT}}$, $n_j = 1/v_j$ and $[-\ln(\sigma/\sigma_{TS})] = \tau$. In Eq. (8a), $j = 1$ when
217 $\sigma/\sigma_{TS} \leq \sigma_1^c$; $j = 2$ when $\sigma_1^c < \sigma/\sigma_{TS} \leq \sigma_2^c$; ... ; $j = p$ when $\sigma/\sigma_{TS} > \sigma_{p-1}^c$ and
218 $\sigma_1^c < \sigma_2^c < \dots < \sigma_{p-1}^c$. σ_j^c are critical values for the normalised stress and so fall between 0
219 and 1. In this approach, there are p creep regimes that occur in distinct ranges for the
220 normalised stress and the p versions of Eq. (8a) then apply to each regime. Typically, p varies
221 between 1 and 4 depending on the material being studied.

222 Next it is proposed that the creep rate ($\dot{\varepsilon}$) equation is of the form

223 $\frac{d\varepsilon}{dt} = \dot{\varepsilon} = (\dot{\varepsilon}_m)^p (1-w)^{n_j} \left(\frac{t}{t_f} \right)^{m_j} = (A_j \tau^{n_j})^p (1-w)^{n_j} \left(\frac{t}{t_f} \right)^{m_j}$ (8b)

224

225 as n_j is negative in value and where m_j are the additional primary creep constants that will be
226 negative in value in the presence of strong primary creep.

227 Re-arranging Eq. (8b) for damage gives

228 $w = 1 - \left(\frac{\dot{\varepsilon}}{(\dot{\varepsilon}_m)^p} \right)^{1/n_j} \left(\frac{t}{t_f} \right)^{-m_j/n_j}$ (9a)

229 Assuming failure occurs when damage reaches some critical value, w_f , where $w_f \leq 1$
230 then,

231 $w_f = 1 - \left(\frac{\dot{\varepsilon}_f}{(\dot{\varepsilon}_m)^p} \right)^{1/n_j}$ (9b)

232 where $\dot{\varepsilon}_f$ is the strain rate at failure. When the minimum creep rate is reached at time t_m , the
233 amount of accumulated damage is greater than zero

234 $w_m = 1 - \left(\frac{\dot{\varepsilon}_m}{(\dot{\varepsilon}_m)^p} \right)^{1/n_j} \left(\frac{t_m}{t_f} \right)^{-m_j/n_j}$ (9c)

235 Next it is proposed that the CDM damage rate (\dot{w}) equation is of the form

236 $\frac{dw}{dt} = \dot{w} = \frac{G_j t^{\chi_j}}{(1-w)^{\phi_j}} t^{m_j}$ (10a)

237 where G_j , χ_j and ϕ_j are additional tertiary damage constants. The indefinite integral of Eq.
 238 (10a) under the assumption that $w = 0$, when $t = 0$ gives

$$239 \quad w = 1 - \left(1 - \frac{(1+\phi_j)G_j\tau^{\chi_j}}{m_j+1} t^{m_j+1} \right)^{\frac{1}{1+\phi_j}} \quad (10b)$$

240 Again, with failure occurring when $w = w_f$,

$$241 \quad \frac{(1+\phi_j)G_j\tau^{\chi_j}}{m_j+1} = \frac{1-(1-w_f)^{1+\phi_j}}{t_f^{m_j+1}} \quad (10c)$$

242 Substituting Eq. (10c) into (10b) gives a simplified expression for damage

$$243 \quad w = 1 - \left(1 + [(1 - w_f)^{1+\phi_j} - 1] \left(\frac{t}{t_f} \right)^{m_j+1} \right)^{\frac{1}{1+\phi_j}} \quad (10d)$$

244 with the time to failure being given by

$$245 \quad t_f = \left[\frac{(m_j+1)(1-(1-w_f)^{1+\phi_j})}{(1+\phi_j)G_j\tau^{\chi_j}} \right]^{\frac{1}{m_j+1}} \quad (10e)$$

246 The Wilshire failure time equation (Eq. (6c)) can be written as

$$247 \quad t_f = e^{\frac{Q_{cj}}{RT}} \left[\frac{1}{k_{1j}} \right]^{u_j} \tau^{\frac{1}{u_j}}$$

248 The failure time equation given by Eq. (10e) is therefore consistent with this Wilshire
 249 time to failure equation, with

$$250 \quad 1/u_j = -\chi_j/(m_j+1) \quad \text{and} \quad \frac{\frac{m_j+1}{\phi_j+1} [(1/k_{1j})^{1/u_j} \exp(Q_{cj}/RT)]^{(1+m_j)}}{1-(1-w_f)^{1+\phi_j}} = 1/G_j \quad (10f)$$

251 Finally, taking the indefinite integral of Eq. (8b) (after substituting in Eq. (10b) or Eq. (10d)
 252 for w) and assuming $\varepsilon = 0$ when $t = 0$ (to determine the constant of integration) gives the
 253 following expressions for the uniaxial creep curve

$$254 \quad \varepsilon = \Gamma \left\{ 1 - \left[\left(\frac{t}{t_f} \right)^{m_j+1} ((1 - w_f)^{1+\phi_j} - 1) + 1 \right]^{\Delta_j} \right\}$$

255 or

$$256 \quad \varepsilon = \Gamma \left\{ 1 - \left[\left(\frac{t}{\left[\frac{(m_j+1)(1-(1-w_f)^{1+\phi_j})}{(1+\phi_j)G_j\tau^{\chi_j}} \right]^{\frac{1}{m_j+1}}} \right)^{m_j+1} ((1 - w_f)^{1+\phi_j} - 1) + 1 \right]^{\Delta_j} \right\} \quad (11a)$$

257

258 where

$$259 \quad \Gamma = \frac{(\dot{\varepsilon}_m)^\rho t_f}{\Delta_j [(1+m_j) - (1+m_j)(1-w_f)^{1+\phi_j}]} = \frac{(A_j \tau^{n_j})^\rho \left[\frac{(m_j+1)(1-(1-w_f)^{1+\phi_j})}{(1+\phi_j)G_j \tau^{\chi_j}} \right]^{\frac{1}{m_j+1}}}{\Delta_j [(1+m_j) - (1+m_j)(1-w_f)^{1+\phi_j}]} \quad (11b)$$

260 and

$$261 \quad \varepsilon_f = \Gamma \left\{ 1 - [(1-w_f)^{1+\phi_j}]^{\Delta_j} \right\} \quad (11c)$$

262 and where $\Delta_j = 1 + \frac{\rho n_j}{1+\phi_j}$.

263 The normalised creep curve is then given by

$$264 \quad \frac{\varepsilon}{\varepsilon_f} = \frac{1 - \left[\left(\frac{t}{t_f} \right)^{m_j+1} ((1-w_f)^{1+\phi_j} - 1) + 1 \right]^{\Delta_j}}{1 - [(1-w_f)^{1+\phi_j}]^{\Delta_j}} = \frac{1 - \left[\left(\frac{t}{\left[\frac{(m_j+1)(1-(1-w_f)^{1+\phi_j})}{(1+\phi_j)G_j \tau^{\chi_j}} \right]^{\frac{1}{m_j+1}}} \right)^{m_j+1} ((1-w_f)^{1+\phi_j} - 1) + 1 \right]^{\Delta_j}}{1 - [(1-w_f)^{1+\phi_j}]^{\Delta_j}} \quad (11d)$$

265

266 4.2. Estimation

267 Estimation requires a mixture of linear and non-linear least squares. The first step
 268 involves estimating the Wilshire equation for the minimum creep rate to obtain values for v_j ,
 269 Q_{cj} and k_{2j} . A hat symbol will be used to designate these as estimates. Details of such a linear
 270 least squares procedure are now well documented in, for example, Evans [15]. Then values
 271 for the parameters A_j and n_j in Eqs. (8b) are estimated as

$$272 \quad \widehat{A}_j = \left[\frac{1}{k_{2j}} \right]^{\frac{1}{v_j}} e^{-\frac{Q_{cj}}{RT}} \quad \text{and} \quad \widehat{n}_j = \frac{1}{v_j} \quad (12a)$$

273 The second step involves testing the assumption that m_j and Δ_j in Eq. (11d) are
 274 temperature dependent. To do this, all the experimental creep curves in the j th creep regime
 275 at temperature 873K are normalised using the measured failure strains. Then w_f is set equal to
 276 1 and non-linear least squares used to estimate the values for m_j and Δ_j in Eq. (11d) at this
 277 temperature and this creep regime. Standard Gauss-Newton algorithms can be used to
 278 minimise the sum of the squared differences between each actual normalised creep strain data
 279 point at 873K in the j th creep regime and that predicted by Eq. (11d). Repeat this process for
 280 all values of w_f in the range 0 – 1 using a simple grid search technique and choose the value
 281 for w_f to be that which gives the smallest such sum of squared differences. Again, let these
 282 estimates be denoted with the hat symbol - \widehat{m}_{jk} , \widehat{w}_{fk} and $\widehat{\Delta}_{jk}$. The subscript k represents
 283 estimates for the k th temperature, and so for the data set in this paper k varies from 1 to 4. By
 284 repeating this process at all the other temperatures and creep regimes, plots of \widehat{m}_{jk} , \widehat{w}_{fk} and
 285 $\widehat{\Delta}_{jk}$ against temperature for each creep regime can be made, and these will then reveal any
 286 dependency on stress and temperature.

287 If there is no dependency on temperature, then m_j and Δ_j can be estimated by
 288 minimising the sum of the squared differences between each actual normalised creep strain
 289 data point at all temperatures in the j th creep regime and that predicted by Eq. (11d). If there
 290 is dependency, then equations need to be found to model this.

291 The third step involves estimating the value for ρ . This parameter is simply the
 292 exponent in the Monkman-Grant relation [26]

$$293 \quad (\dot{\epsilon}_m)^\rho = C \frac{t_f}{\epsilon_f} \quad (12b)$$

294 Estimates for C and ρ are then easily found by regressing the log minimum creep rate
 295 against the log of the ratio of t_f to ϵ_f ($1/\rho$ is the slope of this linear regression line). Let $\hat{\rho}$ be
 296 such an estimate. Assuming no temperature dependency, values for ϕ_j are then found as 1-
 297 $\{(1+\rho n_j)/\Delta_j\}$.

298 The fourth step involves estimating the Wilshire equation for times to failure to
 299 obtain values for $1u_j$ and k_{1j} . Then, and again using the hat symbol to denote parameter
 300 estimates, values for the parameters G_j and χ_j in Eqs. (10a) are given by

$$301 \quad \chi_j = -(\hat{m}_j + 1)/\hat{u}_j \quad \text{and} \quad \frac{\frac{\hat{m}_j + 1}{1 + \hat{\phi}_j} [(1/k_{1j})^{1/\hat{u}_j} \exp(\hat{Q}_{Cj}/RT)]^{(1 + \hat{m}_j)}}{1 - (1 - \hat{w}_f)^{1 + \hat{\phi}_j}} = 1/\hat{G}_j \quad (12c)$$

302 5. Evaluation Statistics

303 Suppose a uniaxial test program is made up of h test conditions (such as one at $\sigma =$
 304 700 MPa with $T = 973K$) and for each test condition some d_i strain-time readings made. Let
 305 ϵ_{it} be the experimental (or actual) value for strain measured at time t and $\hat{\epsilon}_{it}$ the prediction
 306 made for these strains using the Wilshire CDM model described above. Then the accuracy of
 307 the predictions made for these experimental creep curves can be quantified using the mean
 308 percentage squared error (MPSE)

$$309 \quad MPSE = \frac{1}{h \sum_{i=1}^h d_i} \sum_{i=1}^h \sum_{t=1}^{d_i} [(\epsilon_{it} - \hat{\epsilon}_{it})/\epsilon_{it}]^2 \cong \frac{1}{h \sum_{i=1}^h d_i} \sum_{i=1}^h \sum_{t=1}^{d_i} [e_{it}]^2 \quad (13)$$

310 where the $e_{it} = \ln(\epsilon_{it}) - \ln(\hat{\epsilon}_{it})$ are what Holdsworth et. al. [27] termed the residual log
 311 times. The approximation of this residual to the MPSE is better the smaller are the percentage
 312 errors (very close for an error of less than 10%). The standard deviation in these residuals
 313 (labelled S_{A-RLT} by Holdsworth et. al.) can be calculated at each test condition as

$$314 \quad s_{ei} = \frac{1}{d_i - 1} \sum_{t=1}^{d_i} [e_{it} - \bar{e}_i]^2 \quad [14a]$$

315 where \bar{e}_i is the mean residual log time at test condition i . Then, assuming these standard
 316 deviations are independent of test conditions, the standard deviation in the residuals over all
 317 conditions can be estimated as a weighted average of all the s_{ei}

$$318 \quad s_e = \frac{\sum_{i=1}^h [(d_i - 1) s_{ei}]}{\sum_{i=1}^h (d_i - 1)} \quad (14b)$$

319 s_e and MPSE are different because the mean value for e may not be zero – as would be the
 320 case if the model systematically over or underestimates the strain.

321 If the residuals are assumed to be normally distributed (implying strains are log
 322 normally distributed), and the standard deviation for the residuals are independent of stress,
 323 the percentile (p) log strain at test condition i can be calculated

324 $\ln(\varepsilon_i)_p = \ln(\hat{\varepsilon}_i) + s_e z_p$ (15a)

325 where z_p is the p th percentile of the standard normal distribution. Because of the assumed log
 326 normality of the strains, the predicted log strain at test condition i , $\ln(\hat{\varepsilon}_i)$, is actually
 327 interpreted as the median (and therefore mean) log strain at that condition. Then, as an
 328 example, 99% of log strain values will be in the range

329 $\ln(\hat{\varepsilon}_i) \pm s_e 2.58$ (15b)

330 and so 99% of the strain value will be in the range

331 $\hat{\varepsilon}_i e^{\pm s_e 2.58}$ (15c)

332 Holdsworth et. al. [27] have termed $e^{s_e 2.58}$ the Z-parameter and suggested it provides
 333 a means of quantifying model-fitting effectiveness. Ideally, for single-cast analysis, Z should
 334 not exceed 2, whereas Z in excess of 4 is unacceptable [28].

335 However, this interpretation of what is acceptable, assumes that the residual variation
 336 picked up by s_e (and thus Z) is all systematic in nature and so the result of a poorly fitting
 337 creep model. This will not always be the case. Granger and Newbold [29] have shown that

338 $s_e^2 = (\beta - 1)^2 s_{\ln(\hat{\varepsilon})}^2 + s_v^2$ (16a)

339 where $s_{\ln(\hat{\varepsilon})}^2$ is the variance in the predicted log strains, β is the slope of the best fit line on a
 340 cross plot of $\ln(\varepsilon_{it})$ v $\ln(\hat{\varepsilon}_{it})$ and s_v^2 the variance in the residuals around this best fit line
 341 which is given by

342 $\ln(\varepsilon_{it}) = \alpha + \beta \ln(\hat{\varepsilon}_{it}) + v_{it}$ (16b)

343 So part of s_e^2 is caused by β differing from 1, and so by the best fit line being flatter or
 344 steeper than a 45° line on a scatter plot of $\ln(\varepsilon_{it})$ v $\ln(\hat{\varepsilon}_{it})$. This is clearly systematic bias that
 345 is caused by the used creep model itself, because in such a situation the creep model is then
 346 consistently over (or under) predicting $\ln(\varepsilon_{it})$ at low log strains followed by consistently
 347 under (or over) predicting at high log strains - depending on whether β is above or below 1.
 348 On the other hand, v_{it} is clearly random variation with s_v being the standard deviation and
 349 thus size of this random variation.

350 This suggests that a high value for Z would not be an indication of a creep model
 351 making large systematic prediction errors, provided $\beta = 1$. Rather, it would be due to a large
 352 value for s_v . In this extreme situation, all the variation being picked up by Z is purely random
 353 in nature and reflects the stochastic nature of creep in the material under investigation - which
 354 for some materials can result in substantial scatter. The size of this random variation is pre-
 355 determined, and no creep model can reduce it. Instead it is the result of things like
 356 microstructural variation in test samples, accuracy of test equipment etc. At the other
 357 extreme, a large value for Z would be an indicator of a poorly performing creep model if $s_v^2 =$
 358 0 with $\beta \neq 1$.

359 Another issue with Z is that it does not pick up a poorly performing creep model that
 360 is the result of the model failing the predict the log strain even on the average. This can be
 361 seen by noting that the MPSE can also be worked out as

$$362 \quad \text{MPSE} = \bar{\epsilon}^2 + s_{\epsilon}^2 = \bar{\epsilon}^2 + (\beta - 1)^2 s_{\ln(\hat{\epsilon})}^2 + s_v^2 \quad (17a)$$

363 where $\bar{\epsilon}$ is the mean residual over all tests conditions and times. Thus, a proportion of the
 364 MPSE is due to the creep model predicting the strain incorrectly on the average, which is
 365 clearly a systematic error - $U^M = \bar{\epsilon}^2/\text{MPSE}$. This is often referred to as the bias proportion.
 366 Another proportion of the MPSE is due to the regression parameter $\beta \neq 1$, which again is due
 367 to a poorly performing creep model - $U^R = (\beta - 1)^2 s_{\ln(\hat{\epsilon})}^2/\text{MPSE}$. This is often called the
 368 new regression proportion. Finally, a proportion of the MPSE is due to $U^D = s_v^2/\text{MPSE}$ and
 369 is often called the random disturbance proportion. Granger and Newbold have shown that the
 370 last equation can be rewritten as

$$371 \quad \text{MPSE} = \bar{\epsilon}^2 + (s_{\ln(\hat{\epsilon})} - r s_{\ln(\epsilon)})^2 + (1 - r^2) s_{\ln(\epsilon)}^2 \quad (17b)$$

372 where $s_{\ln(\epsilon)}^2$ is the variance in the actual log strains and r the correlation between the actual
 373 and predicted log strains.

374 6. Results

375 6.1. The Wilshire equation for the minimum creep rate

376 The top half of Table 2 shows the least squares estimates made for the parameters of
 377 the Wilshire minimum creep rate equation.

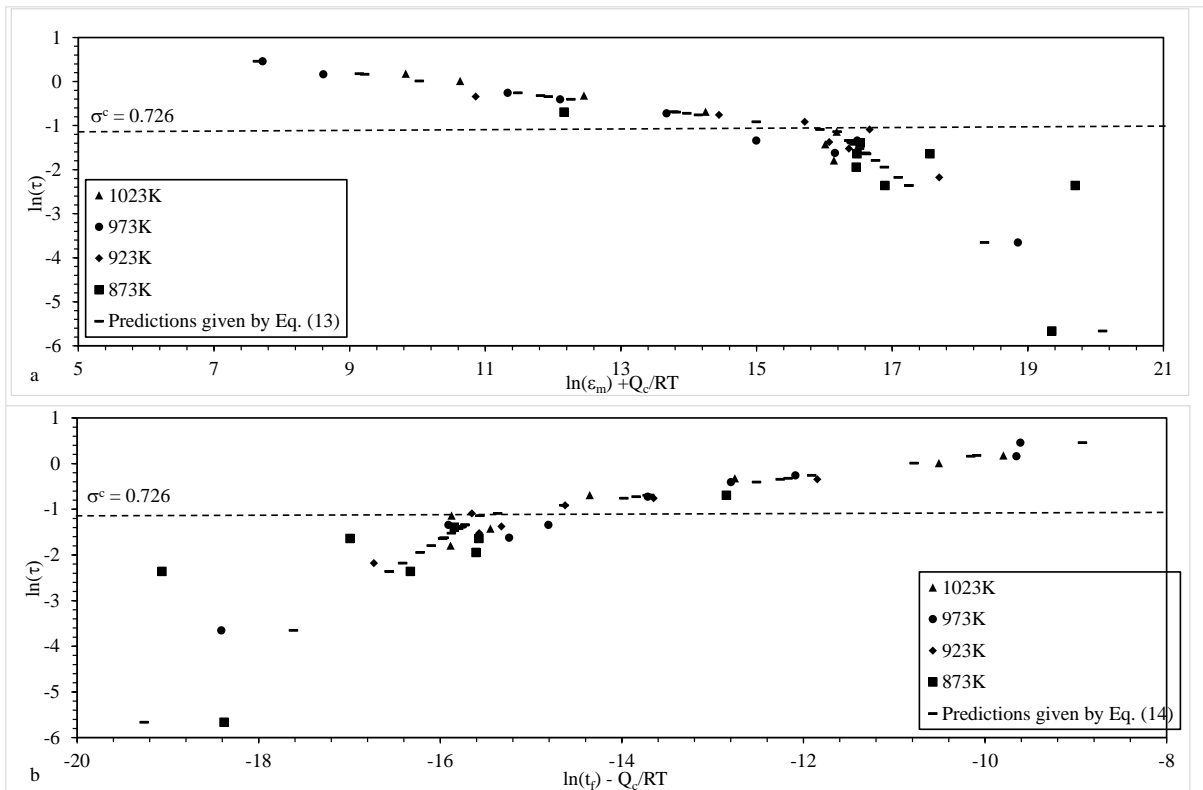
378 Table 2. Estimated parameters of the Wilshire equations

Wilshire minimum creep rate equation – Eq. (8a)		
Parameters	$\sigma/\sigma_{TS} > 0.726$ (j=1)	$\sigma/\sigma_{TS} \leq 0.726$ (j=2)
k_{2j}	42739791.637	6.6002
v_j	-0.8652	-5.3528
$Q_{cj}(\text{Jmol}^{-1})$	225,637	224,432
Wilshire failure time equation – Eq. (6c)		
Parameters	$\sigma/\sigma_{TS} > 0.726$ (j=1)	$\sigma/\sigma_{TS} \leq 0.726$ (j=2)
k_{1j}	60448836.39	13.5687
u_j	0.8168	4.1565
$Q_{cj}(\text{Jmol}^{-1})$	201,529	213,689

379

380 This model is capable of explaining 95.14% of the variation in log minimum creep
 381 rates, and the parameters above and below $\sigma^c = 0.726$ are all statistically significantly
 382 different from each other at the 1% significance level. So, whilst the activation energies
 383 estimated either side of the break stress are only slightly different in value from each other
 384 (224 kJmol^{-1} v 226 kJmol^{-1}), this difference is nonetheless statistically significant at the 1%
 385 significance level. Fig. 1(a) provides a visualisation of this model by plotting $\ln(\tau)$ against
 386 $\dot{\epsilon}_m + Q_c/RT$. There is a clear break in the relationship around $\sigma^c = 0.726$ and all data

387 points seem to fit tightly around the best fit line given by Eqs. (8a) - which is shown as the
 388 dashed line.



389
 390 **Fig. 1.** Dependence of (a) $\ln[\dot{\epsilon}_m \exp(Q_c^*/RT)]$ on $\ln[-\ln(\sigma/\sigma_{TS})]$ and b $\ln[t_f \exp(-Q_c^*/RT)]$
 391 on $\ln[-\ln(\sigma/\sigma_{TS})]$ at various temperatures.

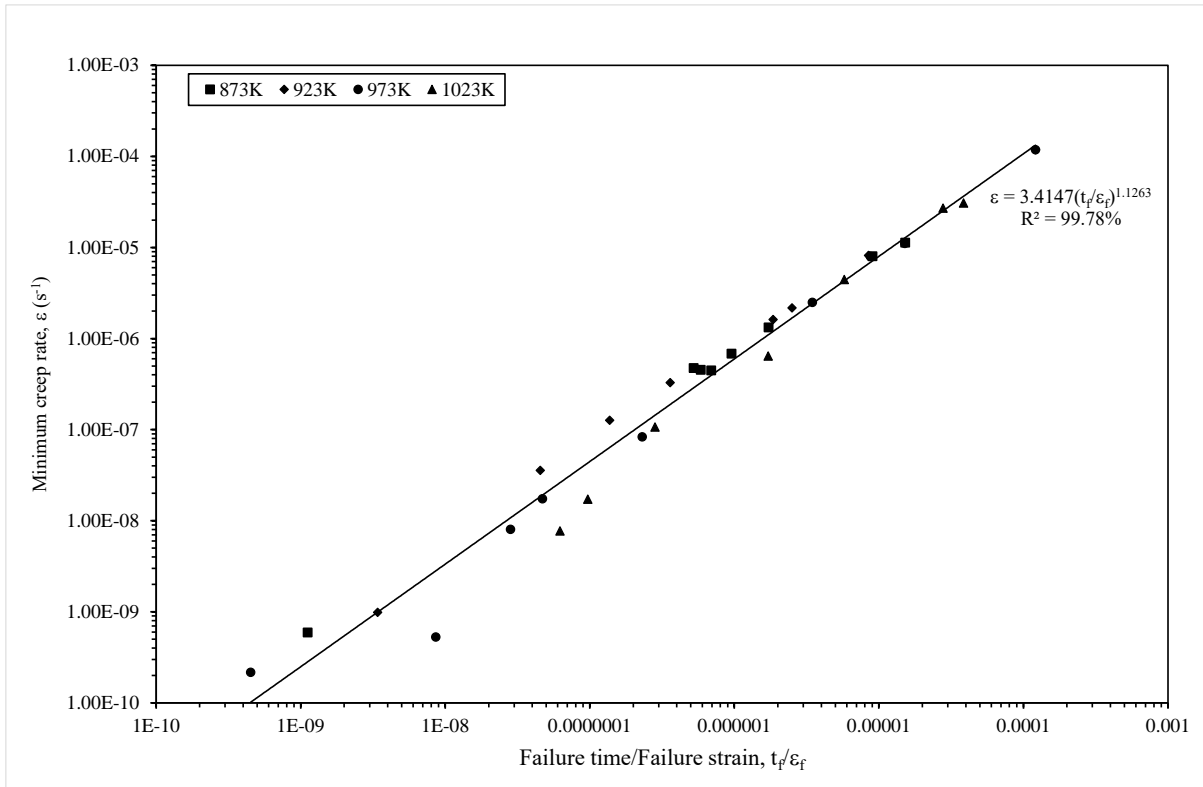
392 It therefore appears that the creep behaviour of Waspaloy is dependent on applied
 393 conditions, with two distinct regions corresponding to stresses above and below σ_Y (the yield
 394 stress which approximately corresponds to a normalised stress of 0.726). This change in
 395 creep behaviour is due to differing mechanisms of creep at different applied conditions.
 396 Whittaker et. al. [9] highlighted the dominance of diffusive climb at stresses below σ_Y with
 397 dislocation-dislocation interaction in the form of forest hardening limiting creep rates at
 398 higher stresses. They showed that geometrically necessary dislocation (GND) densities are
 399 higher at the grain boundaries in Waspaloy samples crept below σ_Y , whereas GND densities
 400 were more uniformly spread through grains in samples crept above σ_Y .

401 6.2. The Wilshire equation for the time to failure

402 The bottom half of Table 2 shows the least squares estimates made for the parameters
 403 of the Wilshire failure time equation. This model is capable of explaining 93.87% of the
 404 variation in log times to failure, and the parameters (with the exception of Q_c) above and
 405 below $\sigma^c = 0.726$ are all statistically significantly different from each other at the 1%
 406 significance level. Fig. 1(b) provides a visualisation of this model by plotting $\ln(\tau)$ against
 407 $t_f - Q_c/RT$. There is a clear break in the relationship around $\sigma^c = 0.726$ and all data the
 408 points seem to fit tightly around the best fit line given by Eqs. (6c) - which is shown as a
 409 dashed line.

410 6.3. The Monkman-Grant relation

411 Fig. 2 shows the least squares estimates of the Monkman – Grant relation, with this
 412 relation explaining 99.78% of the variation in log minimum creep rates. This relationship
 413 gives a good representation of the experimental data irrespective of the temperature, with $\rho =$
 414 $1/1.1263 = 0.8879$ appearing to be independent of temperature.



415
 416 **Fig. 2.** Dependence of minimum creep rate on time to failure and failure strain.

417 *6.4. Analysis at constant temperatures: checking the temperature dependency of Δ_j and m_j*

418 The open circles in Fig. 3 show the experimentally measured creep curves obtained at
 419 873K and for stresses of 900 MPa and above (900, 950, 1000, 1050 and 1150 MPa – with one
 420 replication at 950 and 1050 MPa). This corresponds to the high stress regime identified in sub
 421 sections 4.1 and 4.2 above ($j = 1$). With a UTS of 1154 MPa at this temperature, these
 422 stresses all correspond to values for $\ln(\tau)$ below -1.137. These creep curves have been
 423 normalised using the failure strains and times associated with these measured curves. Now
 424 Eq.(11d) can be thought of as a master normalised creep curve for all tests conditions at or
 425 above 840 MPa and at 873K (i.e. at or above $\sigma/\sigma_{TS} = 0.726$ at 873K). Table 3 shows the
 426 estimates made for the parameters m and Δ of this master curve using non-linear least
 427 squares.

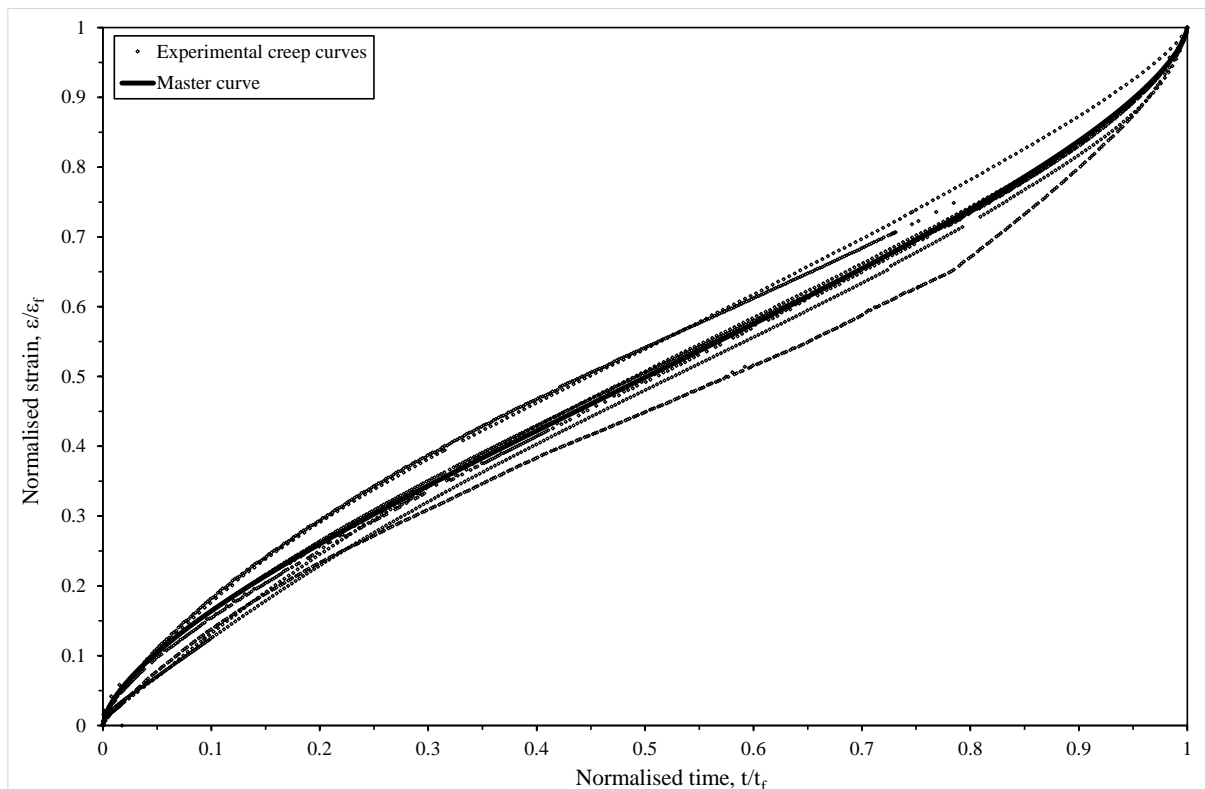
428
 429
 430
 431

432 Table 3 Parameters in the Wilshire CDM creep curve of Eq. (11a,b) and for use at a
 433 temperature of 873K with stresses above 840 MPa (i.e. $j = 1$).

Parameters	Calculation Method	Estimate
m_1		-0.3765
	Application of non-linear least squares to Eq. (11d)	
Δ_1		0.6592
n_1	Calculated from the values for v_1 in Table 2 using Eqs. (8a,12a)	-0.8652
A_1	Calculated from v_1, k_{21} and Q_{c1} in Table 2 using Eqs. (8a,12a)	6.8001E-07
G_1	Calculated from u_1, k_{11}, Q_{c1} in Table 2 and m_1, ϕ_1 using Eqs. (10f,12c)	1.5889E-06
χ_1	Calculated from m_1 and u_1 in Table 2 using Eqs. (10f,12c)	-0.7893
ρ	Exponent in the Monkman-Grant relation in Fig. 2	0.8879
ϕ_1	Derived from n_1, Δ_1 and ρ - see Eq. (11c)	1.2541

434

435 Using these values with $w_f = 1$ yields the master curve in Fig. 3 shown as the solid
 436 black curve. This curve appears to present the shape of the normalised experimental creep
 437 curves well.



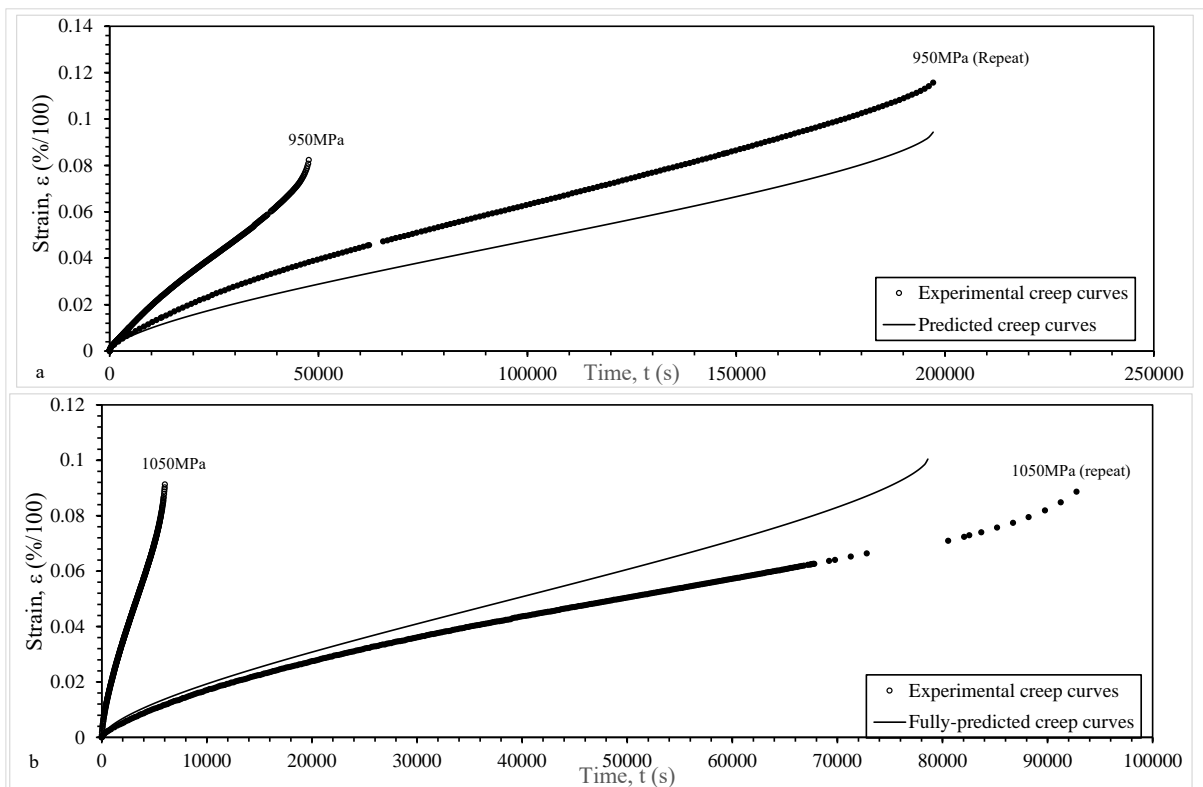
438

439 **Fig. 3.** Normalised experimental creep curves obtained at 873K and for stress at or above 900
 440 MPa, together with the predicted master curve given by Eq. (11d).

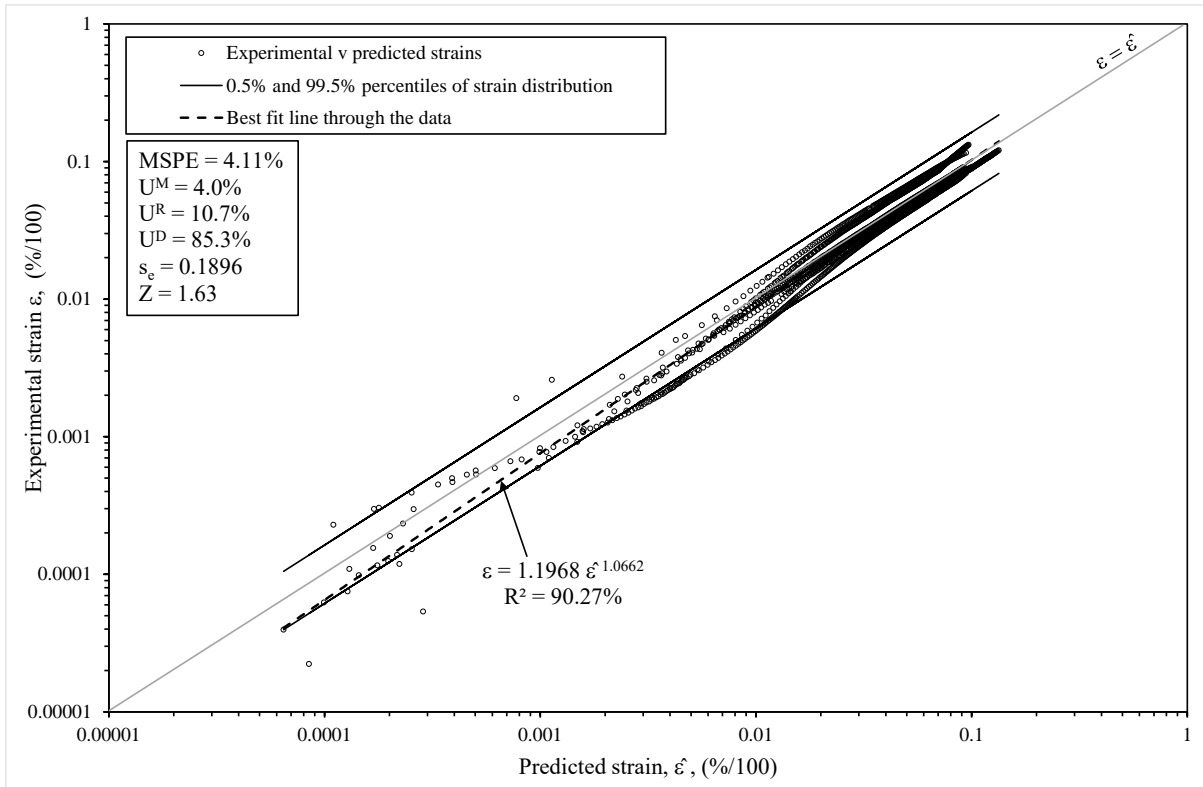
441 This master curve can then be used to predict actual creep curves. This can be done by
 442 rescaling the master curve using the values for Γ in Eq. (11b), which in turn are calculated
 443 from the remaining parameters shown in Table 3. Fig. 4(a,b) shows some creep curves
 444 calculated in this way. In Fig. 4(a) the two creep curves measured at 873K and 950 MPa are
 445 shown together with the predicted creep curve for this test condition. The predicted curve is
 446 closer to one of the measured curves, but the figure also clearly demonstrates the large

447 random or stochastic component of creep that is present for this alloy. In Fig. 4(b) the
 448 predicted creep curves is in between the two measured creep curves at 1050 MPa. Again, the
 449 stochastic nature of creep is clearly visualised.

450 The full accuracy of the predictions made for the recorded creep curves obtained at
 451 873K and for stresses of 900 MPa or more is shown in Fig. 5. Here the actual strains are
 452 plotted against the predicted strains obtained using Eqs. (11a,b) on a (natural) log scale and
 453 so a perfect model would correspond to all data points falling on the shown 45^0 line. The Z
 454 parameter of 1.63 is below the minimum acceptable value suggested by Holdsworth et. al.
 455 and implies that 99% of all strains will fall within the range of 1.63 times the predicted strain.
 456 The shape of the creep curves appears to be well predicted at low and high strains, but at
 457 intermediate strains the predictions tend to underestimate the actuals creep strains. The mean
 458 percentage squared error (MPSE) is equal to 4.11% (with a root MPSE of just over 2%).
 459 Further, 4% of this MPSE is attributable to the squared difference between the average strain
 460 and the predicted strain. An additional 10.7% of this MPSE is attributable to the best fit line
 461 shown in Fig. 5 being a little steeper than the ideal 45^0 line, implying a small tendency of the
 462 Wilshire CDM model to systematically under predict at low strains and then over predict at
 463 higher strains. Both these components of the MPSE represent systematic errors made in
 464 predicting the actual creep curves at 873K and so this source of error amounts to some 15%
 465 of the MPSE. The remaining 85% of the MPSE is by deduction random (and so
 466 unpredictable) in nature and simply reflects the stochastic nature of creep in Waspaloy - as is
 467 evident in Figs (4).



468
 469 **Fig. 4.** Experimental creep curves obtained at 873K together with predicted curves given by
 470 Eqs. (11a,b) when (a) stress =950 MPa and (b) when stress = 1050 MPa.

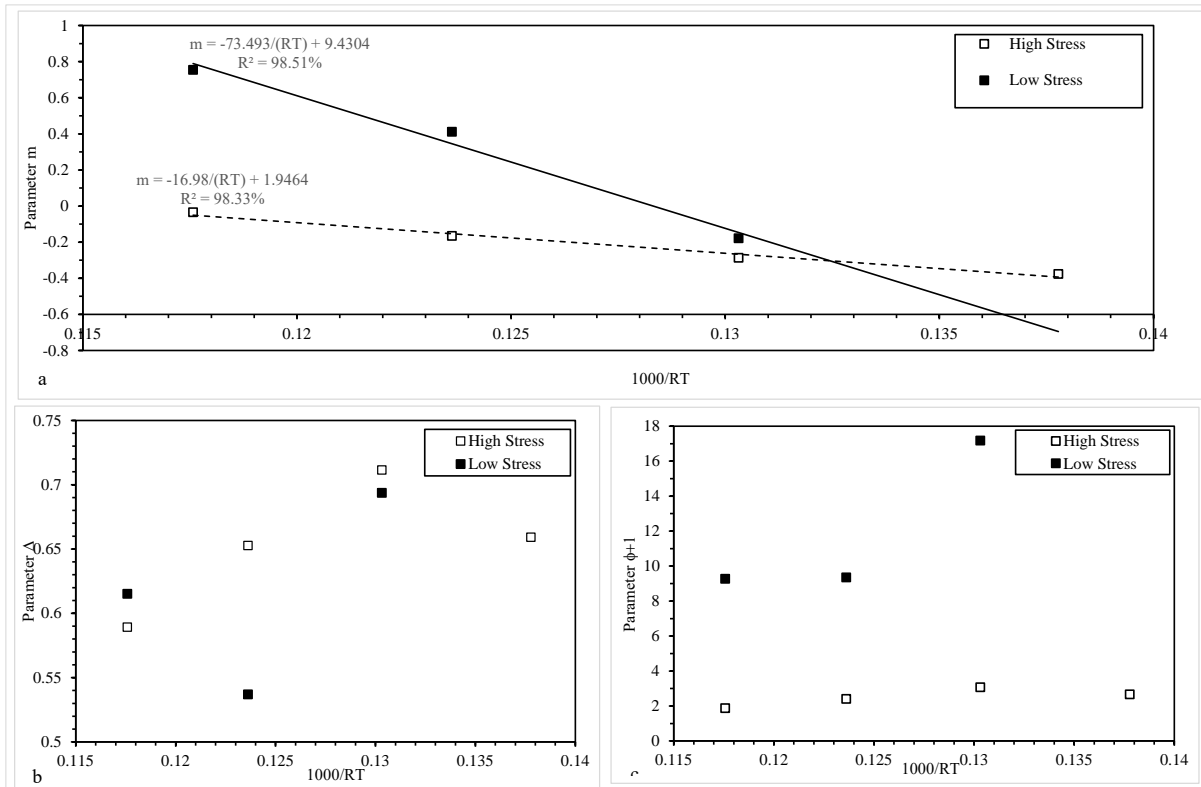


471

472 Fig.5. Plot of actual against predicted creep curves at 873K and at normalised stresses above
 473 0.726.

474 Fig. 6 shows the results of repeating the above analysis at the other temperatures –
 475 both above and below the break point stress (as there is only 1 data point below σ^c at 873K
 476 no such an analysis could be done for these test conditions). It is clear from this figure that
 477 the parameter m is always higher in the lower stress regime (although the gap diminishes
 478 with decreasing temperature). In this low stress regime, m is also always positive implying
 479 there is no or very short-lived primary creep. In contrast, in the higher stress regime, m is
 480 always negative so that more pronounced primary creep occurs irrespective of the
 481 temperature. Irrespective of the stress regime, there is a tendency for m to reduce in size as
 482 the temperature decreases. Whilst ϕ is clearly higher in the low stress regime, there is no
 483 strong evidence to suggest that ϕ varies systematically with temperature. For the parameter Δ ,
 484 there is again no strong evidence to suggest it varies either with stress or temperature.

485



486

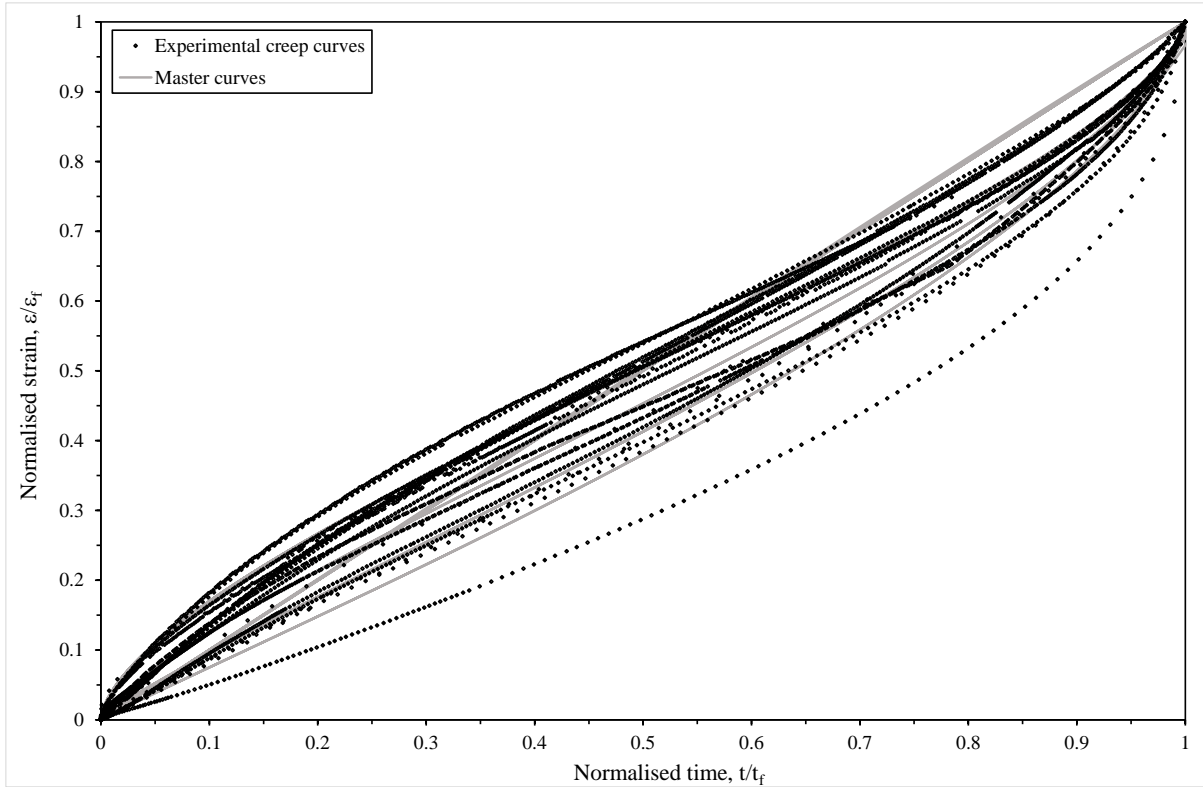
487 **Fig. 6.** Variations of (a) parameter m , (b) parameter Δ and (c) parameter ϕ with temperature
 488 and creep regime (low and high stress regimes).

489 Based on these results it seems sensible to assume that Δ and ϕ are independent of
 490 temperature, but m requires some additional modelling. In this paper, the dependence of m on
 491 temperature was modelled as a linear function of $1000/RT$ – as seen in Fig. 6(a)

492 *6.5. Combining temperatures in the high stress regime .*

493 The results above suggest the model can be used to predict creep curves at any
 494 temperature by treating Δ as fixed and modelling the parameter m using the linear expression
 495 shown in Fig. 6(a). Thus $m+1$ varied from 0.62 at 873K through to 0.97 at 1023K for
 496 normalised stresses in excess of 0.726. This implies that there is a well-defined primary creep
 497 stage present within the creep curves at these conditions, with this stage become less defined
 498 with increasing temperature. The open circles in Fig. 7 show the experimentally measured
 499 creep curves obtained at all temperatures and for all stresses in the high stress regime, (i.e. for
 500 $\sigma^c > 0.726$). These creep curves have been normalised using the failure strains and times
 501 associated with these measured curves. Using all such test conditions, and using $w_f = 1$, the
 502 non-linear least squares estimate for Δ_1 was found to be 0.6567 - and so not to different from
 503 the value obtained at 873K.

504 This Δ value and the temperature dependant values for m resulted in the master curves
 505 shown in Fig. 7 – represented as the solid grey curves and they appear to present the shape of
 506 the normalised experimental creep curves reasonably well. There is one master curve for each
 507 temperature as the parameter m changes with temperature.



508

509 **Fig. 7.** Normalised experimental creep curves obtained at 873-1023K and for higher stresses
 510 corresponding to $\sigma_c < 0.726$, together with the predicted master curves given by Eq. (11d).

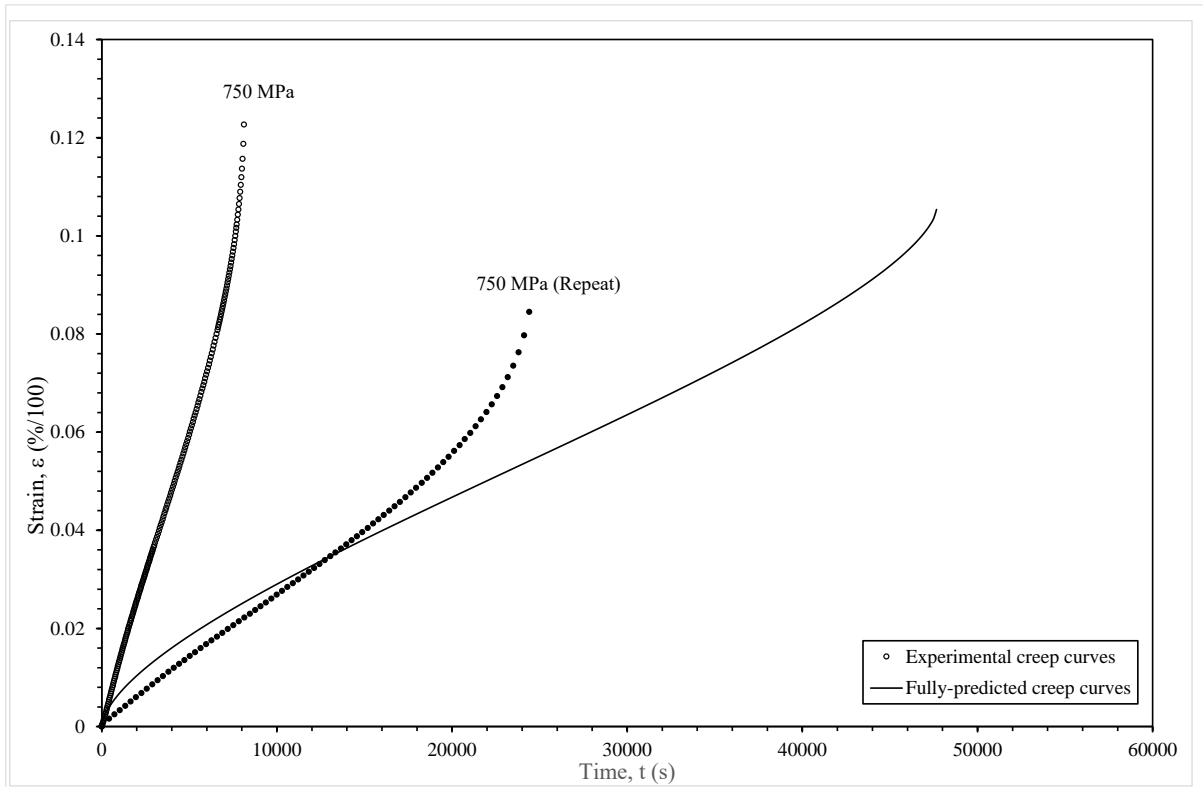
511 Table 4 gives the parameters of Eq. (11a,b) that can be used to predict creep curves at
 512 the four shown temperatures and normalised stresses above 0.726. Fig. 8 shows one such
 513 predicted creep curve obtained at 973K and 750 MPa, together with the creep curves
 514 associated with the two specimens placed on test at this condition. Again, the highly
 515 stochastic nature of creep in this material is present and the predicted creep curve is a better
 516 fit at the earlier strains.

517 Table 4 Parameters in the Wilshire CDM creep curve of Eq. (11a,b) and for use at a
 518 temperatures of 873K, 923K, 973K and 1023K and with normalised stresses above 0.726 (i.e.
 519 $j = 1$).

Parameters	Estimates				
	All temperatures	873K	923K	973K	1023K
m_1	-	-0.393	-0.2663	-0.1526	-0.05
Δ_1	0.6567	-	-	-	-
n_1	-0.8652	-	-	-	-
A_1	-	1.2623E-07	6.8001E-07	3.0812E-06	1.2044E-05
G_1	-	8.0552E-05	5.5586E-05	5.3705E-05	6.6693E-05
χ_1	-	-0.4957	-0.5993	-0.6921	-0.7759
ρ	0.8879	-	-	-	-
ϕ_1	1.6065	-	-	-	-

520

521



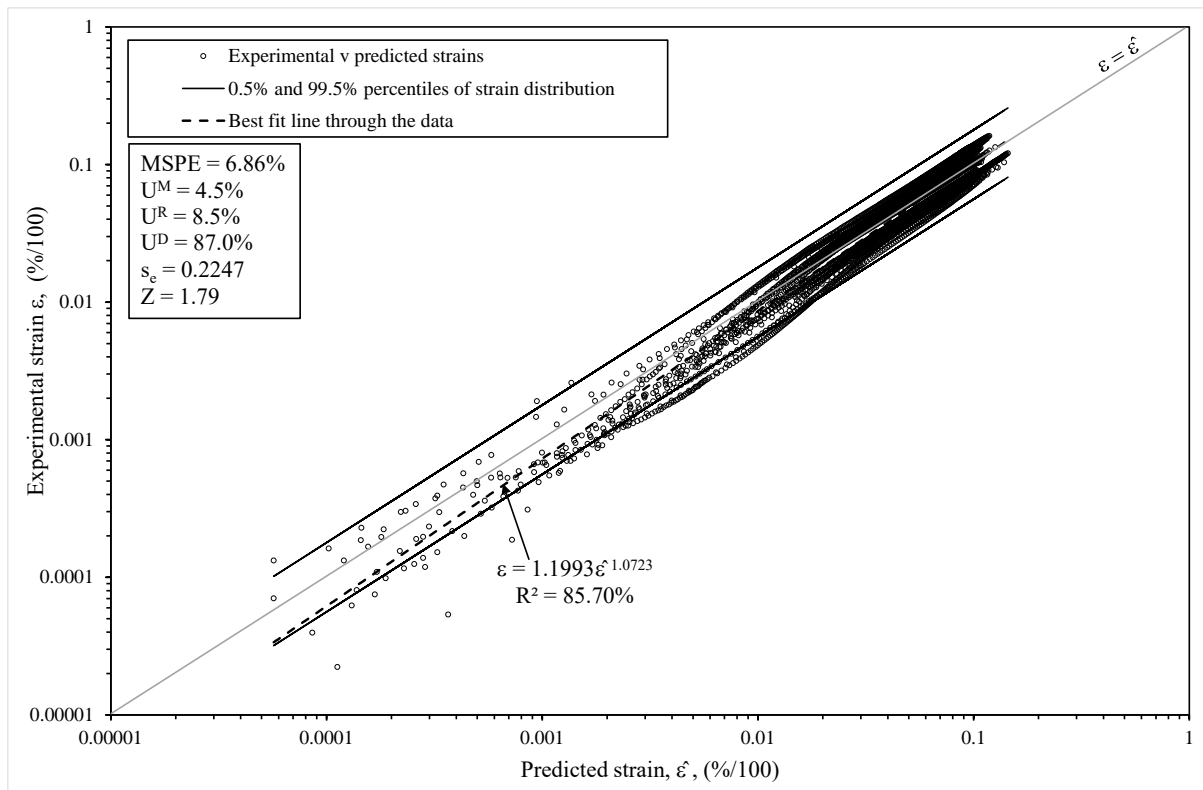
522

523

524 **Fig. 8.** Experimental creep curves obtained at 973K and 750 MPa, together with predicted
 525 curve given by Eqs. (11a,b).

526 The full accuracy of the predictions made for the recorded creep curves obtained at
 527 873K – 1023K and for normalised stresses of 0.726 is shown in Fig. 9. Here the actual strains
 528 are plotted against the predicted strains obtained using Eqs. (11a,b) on a (natural) log scale
 529 and so a perfect model would correspond to all data points falling on the shown 45° line. The
 530 Z parameter of 1.79 is below the minimum acceptable value suggested by Holdsworth et. al.
 531 and implies that 99% of all strains will fall within the range of 1.79 times the predicted strain.
 532 The shape of the creep curves appears to be well predicted at low and high strains, but at
 533 intermediate strains the predictions tend to underestimate the actuals creep strains. The mean
 534 percentage squared error (MPSE) is equal to 6.86% (with a root MPSE of just over 2.62%).
 535 Further, 4.5% of this MPSE is attributable to the squared difference between the average
 536 strain and the predicted strain. An additional 8.5% of this MPSE is attributable to the best fit
 537 line shown in Fig. 9 being a little steeper than the ideal 45° line, implying a small tendency of
 538 the Wilshire CDM model to systematically under predict low strains and then over predict at
 539 higher strains. Both these components of the MPSE represent systematic errors made in
 540 predicting the actual creep curves at these conditions and so this source of error amounts to
 541 some 13% of the MPSE. The remaining 87% of the MPSE is by deduction random (and so
 542 unpredictable) in nature and simply reflects the stochastic nature of creep in Waspaloy as was
 543 evident in Figs (4,8).

544



545

546 **Fig. 9.** Plot of actual against predicted creep curves at 873K – 1023K and at normalised
 547 stresses above 0.726.

548 **7. Conclusions**

549 This paper integrated the Wilshire failure time and minimum creep rate equations into
 550 a modified Kachanov-Rabotnov CDM creep model that was capable of modelling both
 551 primary and tertiary creep. The paper also presented an estimation strategy for the unknown
 552 parameters of this model. This CDM model was then applied to uniaxial creep data on
 553 Waspaloy. It was found that the Wilshire equations provided very good fits to the data on
 554 times to failure and minimum creep rates. Two different creep regimes were identified using
 555 these equations – with a change in creep regime appearing to take place at a normalised stress
 556 of 0.726. The activation energy, whilst statistically significantly different either side of this
 557 stress, was not very different in value. Following other authors, it was hypothesised that this
 558 break was due to a dominance of diffusive climb at stresses below σ_Y , with dislocation-
 559 dislocation interaction in the form of forest hardening limiting creep rates occurring at higher
 560 stresses.

561 The parameter m of the CDM model was found to be stress and temperature
 562 dependent, such that at the lower temperatures m is clearly negative implying well defined
 563 tertiary creep. This stage of creep then tends to disappear at higher temperatures (as m tends
 564 to zero at these temperatures). The parameter Δ was found to be broadly independent of the
 565 temperature. Finally, the CDM model was shown to be reasonably accurate at predicting the
 566 experimental creep curves. At 873K the root MPSE was just over 2%, whilst the model
 567 applied to all temperatures had a root MPSE of 2.6%. In both these illustrations the vast
 568 majority of the prediction errors were random in nature. The scatter, as measured by the Z
 569 parameters, were below 2 in both instances

570 Some areas for future research include the application of this model to other high
571 temperature materials, to assessing the models ability to predict creep curve shape at
572 conditions not used in estimating the models unknown parameters and the incorporation of
573 the Wilshire equations into multiple damage parameter CDM models.

574 **Data Statement**

575 The data used in this paper has been in the public domain for a number of years as shown in
576 the reference section. Data can be made available from the author upon request.

577 **References**

- 578 [1] P. Ruffles, *Aerospace Structural Materials: Present and Future*, (1995) The Institute of
579 Materials London.
- 580 [2] Materials UK Energy Review: Report 1, *Energy Materials – Strategic Research*
581 *Agenda*, 2007.
- 582 [3] B. Wilshire, A.J. Battenbough, Creep and creep fracture of polycrystalline copper.
583 *Materials Science and Engineering A*, 443 (2007) 156-166.
- 584 [4] B. Wilshire, P. J. Scharning, Prediction of long term creep data for forged 1Cr-1Mo-
585 0.25V steel, *Materials Science and Technology*, 24(1) (2008) 1-9.
- 586 [5] B. Wilshire, M. Whittaker, Long term creep life prediction for Grade 22 (2.25Cr—
587 1Mo) steels, *Materials Science and Technology*, 27(3) (2011) 642-647.
- 588 [6] M. Evans, Incorporating specific batch characteristics such as chemistry, heat
589 treatment, hardness and grain size into the Wilshire equations for safe life prediction in
590 high temperature applications: An application to 12Cr stainless steel bars for turbine
591 blade, *Applied Mathematical Modelling*, 40(23-24) (2016) 10342-10359.
- 592 [7] B. Wilshire, P. J. Scharning, A new methodology for analysis of creep and creep
593 fracture data for 9–12% chromium steels, *International Materials Reviews*, 53(2)
594 (2008) 91-104.
- 595 [8] M. T. Whittaker, M. Evans, B. Wilshire, Long-term creep data prediction for type 316H
596 stainless steel. *Materials Science and Engineering A*, 552 (2012) 145-150.
- 597 [9] M. T. Whittaker, W. Harrison, C. Den , C. Rae , S. Williams, Creep Deformation by
598 Dislocation Movement in Waspaloy, *Materials*, 10(1) (2017) 61.
- 599 [10] B. Wilshire, P. J. Scharning, Extrapolation of creep life data for 1Cr-0.5Mo Steel, *Int. J.*
600 *Press. Vessel. Pip.*, 85 (2008) 739–743.
- 601 [11] M. T. Whittaker, W. J. Harrison, R.J. Lancaster, S. Williams, An analysis of modern
602 creep lifing methodologies in the Titanium alloy Ti6-4, *Mater. Sci. Eng. A*, 577 (2013)
603 14–119.
- 604 [12] W. Harrison, M. T. Whittaker, S. Williams, Recent Advances in Creep Modelling of
605 the Nickel Base Superalloy, Alloy 720Li, *Materials*, 6 (2013) 1118–1137.

- 611 [13] Z. Abdallaha, K. Perkins, S. Williams, Advances in the Wilshire extrapolation
612 technique—Full creep curve representation for the aerospace alloy Titanium 834,
613 *Materials Science and Engineering: A*, 550(30) (2012) 176-182.
- 614 [14] V. Gray, M .T. Whittaker, Development and Assessment of a New Empirical Model for
615 Predicting Full Creep Curves, *Materials*, 8, (2015) 4582-4592.
616
- 617 [15] M. Evans, T. Williams, Assessing the capability of the Wilshire equations in predicting
618 uniaxial creep curves: an application to Waspaloy, *Int. J. Pres. Ves. Pip.* 172 (2019)
619 153–165.
- 620 [16] J. A. Cano, C. M. Stewart. A continuum damage mechanics (CDM) based Wilshire
621 model for creep deformation, damage, and rupture prediction, *Materials Science and*
622 *Engineering: A*, 799 (2021).
623
- 624 [17] R.W. Evans, B. Wilshire, *Introduction to Creep*, 1st Edition, (1993) Institute of
625 Materials, London 23–28.
- 626 [18] B. Wilshire, P.J. Scharning, Theoretical and practical approaches to creep of Waspaloy,
627 *Materials Science & Technology*, 25(2) (2009) 242-248.
- 628 [19] R.W. Evans, A constitutive model for the high-temperature creep of particle-hardened
629 alloys based on the θ projection method, *Proceedings of the Royal Society London - A*,
630 456 (2000) 835-868.
- 631 [20] L.M. Kachanov, Rupture Time Under Creep Conditions, *Int. J. Fract.*, 97 (1999) 11–
632 18.
- 633 [21] Y.N. Rabotnov, *Creep Problems in Structural Members*, (1969) North-Holland
634 Publishing, Amsterdam, The Netherlands.
- 635 [22] D.R. Hayhurst, B.F Dyson, J. Lin, Breakdown of the skeletal stress technique for
636 lifetime prediction of notched tension bars due to creep crack growth. *Engineering*
637 *Fracture Mechanics*, 49(5) (1994) 711–726.
- 638 [23] D.R. Hayhurst, Creep continuum damage mechanics: A unifying theme in high
639 temperature design, *High Temperature Structure Design*, ESIS 12, Edited by L. H.
640 Larsson, Mechanical Engineering Publications, London, 3 (1992) 17-334.
- 641 [24] M.S. Haque, C.M. Stewart, 2016, Finite-Element Analysis of Waspaloy using Sinh
642 Creep-Damage Constitutive Model Under Triaxial Stress State, *ASME J. Pressure*
643 *Vessel Technol.*, 138(3), (2016) 031408.
- 644 [25] Y. Liu, S. Murakami, Damage localization of conventional creep damage models and
645 proposition of a new model for creep damage analysis, *JSME International Journal*
646 *Series A*, 41(1) (1998) 57–65.
- 647 [26] D. C. Dunand, B.Q. Han and A.M. Jansen: Monkman-Grant analysis of creep fracture
648 in dispersion-strengthened and particulate-reinforced aluminium, *Metallurgical and*
649 *Materials Transactions A*, 30(13) (1999) 829-838.

650 [27] S.R. Holdswortha, M. Askinsb, A. Bakerc, E. Gariboldi, S. Holmströme, A. Klenkf, M.
651 Ringelf, G. Merckling, R. Sandstromh, M. Schwienheeri, S. Spigarellij, Factors
652 influencing creep model equation selection, *International Journal of pressure Vessels*
653 *and Piping*, 5 (2008) 80–88.

654 [28] S.R. Holdsworth, Developments in the assessment of creep strain and ductility data,
655 *Mater. High Temp.*, 21(1) (2004) 125–32

656 [29] C. Granger, P. Newbold, Some comments on the evaluation of economic forecasts,
657 *Applied Economics*, 5 (1973) 35-47.

658 [30] H. Theil, *Applied Economic Forecasts*, (1966) Amsterdam North Holland.

659

660

661

662

663

664

665

666

667

668

669

670

671

672

673

674

675

676

677

678

679

680

681

Nomenclature	
T	Temperature (K)
σ	Stress (MPa)
σ_{TS}	Ultimate tensile strength (UTS)
w, \dot{w}, w_f	K-R damage parameter, rate of damage accumulation, damage at failure
τ	Transformed and normalised stress, $[-\ln(\sigma/\sigma_{TS})]$
σ^c	Critical values for the normalised stress in the Wilshire models
t	Time (s)
t_f	Time at failure
ε	Strain
ε_f	Strain at failure
$\dot{\varepsilon}$	Strain rate
$\dot{\varepsilon}_m$	Minimum creep rate
A, δ, ϕ, n, χ	Parameters of the K-R and Wilshire CDM models
m	Additional parameter of the Hayhurst extension of the K-R model
k_1, u	Parameters of the Wilshire failure time equation
k_2, v	Parameters of the Wilshire minimum creep rate equation
Q_c	Activation energy for self diffusion
C, ρ	Monkman- Grant parameters
G	Additional Parameter of the Wilshire CDM model
h	Number of separate test conditions in test matrix
m_i	Number of strain-time readings made at test condition i
ε_{it}	Strain recorded at time t under test condition i
$\hat{\varepsilon}_{it}$	Strain predicted by the Wilshire CDM model at time t under test condition i
e_{it}	Residual log times
MPSE	Mean percentage squared error
\bar{e}	Mean residual log time over all test conditions
\bar{e}_i	Mean residual log time at test condition i
s_{ei}	Standard deviation in these residual log times at test condition i
s_e	Standard deviation in these residual log times at all test conditions
z_p	Percentile of the standard normal distribution
Z	Parameter quantifying effectiveness of a creep model to predict strain
$s_{\ln(\hat{\varepsilon})}^2$	Variance in the predicted log strains
S_v^2	Variance in the residual log times
$s_{\ln(\varepsilon)}^2$	Variance in the log strains
r	Correlation between actual and predicted log strains
α, β	Parameters of a best fit line for $\ln(\varepsilon)$ v $\ln(\hat{\varepsilon})$
U^M, U^R, U^D	Proportions of the MPSE
Γ, K	Variables for un-normalised the master normalised creep curve
$\ln(\varepsilon_i)_p$	Percentile of the log strain .
σ_t and σ_s	Additional material constants in the model by Haque [24]
$\dot{\varepsilon}_f$	Creep rate at failure
\dot{w}_f/\dot{w}_0	Ratio of the final to initial rates of damage accumulation